Monitoring subfield level nitrogen requirements for winter wheat and spring barley based on crop yield predictions, remote sensing imagery and soil texture maps

Natalie Hollain[1], Sheng Wang[1], Birgitte Feld Mikkelsen[2], René Gislum[1]

[1] Institute for Agroecology, Aarhus University, Denmark

[2] DanishAgro, Galten, Denmark

A paper from the Proceedings of the
17th International Conference on Precision Agriculture and 11th Brazilian Congress on Precision and Digital Agriculture
13-15 July 2026
Porto Alegre, Brazil

Abstract.

To maximize farmers' contribution margin while simultaneously minimizing nitrogen fertilization, the timely and accurate evaluation of crop nitrogen demand is essential. Fine-grained information about the yield and nitrogen status of fields must be available to perform optimal fertilization. This paper introduces a novel nitrogen monitoring approach that assesses nitrogen requirements within-field (i.e. at the subfield level). The key idea behind the approach is that nitrogen demands can be approximated from the ***prediction-expectation (PE) yield gap****: the difference between predicted and expected crop yield. The PE yield gap serves as a proxy for the nitrogen demand. Crop yield predictions at a 10 x 10 m^2 resolution are obtained from a U-Net model trained on spectral, weather, soil and topography data. The model provides in-season predictions approximately 2 – 3 months before harvest. The expected yield is computed based on expert judgments that take into account the crop type and fine-grained soil conditions within the field.*

We present a case study of our approach for Denmark, where the government is expected to implement a new quota-based, farm-level nitrogen regulation for farmers. Data for over 350 winter wheat and barley fields were collected to demonstrate our novel nitrogen monitoring approach. For crop yield prediction, the U-Net model achieves R2 values of 0.576/0.530/0.506, RMSE of 1.878/2.010/2.186, and MAE of 1.474/1.544/1.702 on the train/validation/test data, demonstrating robust performance across all data splits. Expert judgments were obtained from a recent government report and were used to calculate the expected yield at the subfield level. To demonstrate our nitrogen monitoring approach in action, we selected an example field and illustrated that fertilization can be increased only where necessary, rather than uniformly applying the same fertilizer rate across the entire field. This work serves as a proof of concept for our approach, and we hope it can be adapted to broader contexts to support future advancements in the field.

Keywords.
Nitrogen Management, Fertilizer Optimization, Crop Yield Estimation, Machine Learning, Precision Agriculture

Introduction

The timely and precise evaluation of crop nitrogen demand is crucial for maximizing farmers' contribution margin while simultaneously minimizing nitrogen fertilization. Sufficient nitrogen fertilizer must be provided for adequate crop growth, yet fertilization should not be excessive to minimize its environmental impact (Zhou, et al., 2025). A variety of factors determine both nitrogen demands and crop yield, including weather, topography and soil texture (Balasubramanian, et al., 2004; Kumhálová, et al., 2011). These factors vary spatially, meaning that different amounts of fertilizer may be optimal even across a single field. High resolution satellite remote sensing imagery provides a non-invasive manner of assessing these properties at a resolution of a few meters. Previous work has leveraged multimodal remote sensing data to estimate either crop yield prediction or nitrogen status (Mena, et al., 2025; Zhou, et al., 2026). Few approaches focus on both simultaneously, and those that do are typically limited to small-scale, field-level studies (Wang, et al., 2021; Guo, et al., 2026). To perform variable-rate fertilization within fields, it is paramount that subfield level information about both the yield and nitrogen status is available.

This paper introduces a novel approach that monitors nitrogen requirements precisely within a field. The approach makes use of the assumption that in-field nitrogen demand can be gauged by comparing accurate, in-season yield predictions to expert judgments of the expected yield. The **prediction-expectation (PE) yield gap** between the predicted and expected yield provides insight into the fertilization needed to reach the crop's full growth potential. We train a U-Net model to predict subfield level yield approximately 2 – 3 months before harvest, using remotely sensed weather, soil, topography and spectral data from publicly available sources. The expected yield is derived from judgments by agricultural experts and takes into account soil conditions and crop type. Using the PE yield gap, i.e. the difference between the expected and predicted yield values, we produce nitrogen sufficiency maps to detect areas within fields that require additional fertilization. By providing timely in-season estimates, we demonstrate how precise management of fertilizer application in fields at a subfield level can be performed.

We present a case study of our approach for winter wheat and spring barley fields in Denmark, where the government is expected to implement a new nitrogen regulation for farmers. The regulation is based on a farm-level, quota-based system and restricts nitrogen discharges into coastal waters. This requires detailed mapping of soil characteristics and leaching potential to set individual farm quotas. Danish farmers must therefore optimize their nitrogen use efficiency, both between and within fields. Yield data for over 350 Danish winter wheat and spring barley fields were collected and used to illustrate our novel nitrogen monitoring approach.

Methodology

This paper provides a case study of monitoring nitrogen requirements at the subfield level. By monitoring nitrogen demands at a high spatial resolution, we aim to help farmers make targeted fertilizer applications across their fields. Our approach is as follows. First, we train a U-Net model (Ronneberger, et al., 2015) to predict yield at a resolution of 10 meters. Predictions must be timely to allow farmers to adjust fertilization and meet nitrogen demands. Nitrogen is typically applied two to four times during the growing season, and adjustments can be made to the rate at each application. The model is thus trained to predict yield approximately 2 – 3 months before harvest, when predictions remain actionable for adjusting fertilizer applications. From there, we estimate the nitrogen demand across the field based on the gap between the potential and predicted yield. The potential yield is derived from expert judgments. In the following sections, the study setup is described in more detail.

Study site

This work focuses on spring barley and winter wheat across Denmark. These crops are among the most widely grown in the country and thus represent typical local agricultural practices. Additionally, the growth cycles of spring barley and winter wheat overlap between spring and autumn of a given year, such that they can be jointly monitored during this period. In Denmark, both crops are harvested approximately between early and late August, further motivating the choice to focus on these two crops simultaneously.

Observations across 184 and 204 fields were collected for 2024 and 2025, respectively. In total, 388 fields were studied. The number of winter wheat fields was 68 in 2024, and 105 in 2025, whereas the number of spring barley fields was 116 in 2024, and 99 in 2025. Fields were selected from across the entire country to ensure a varied and representative sample of the growing conditions of Denmark. **Figure 1** visualizes the spatial distribution of the fields and the distribution of field size. Fields ranged in size from 1 to 232 hectares, with the median being 30 hectares.

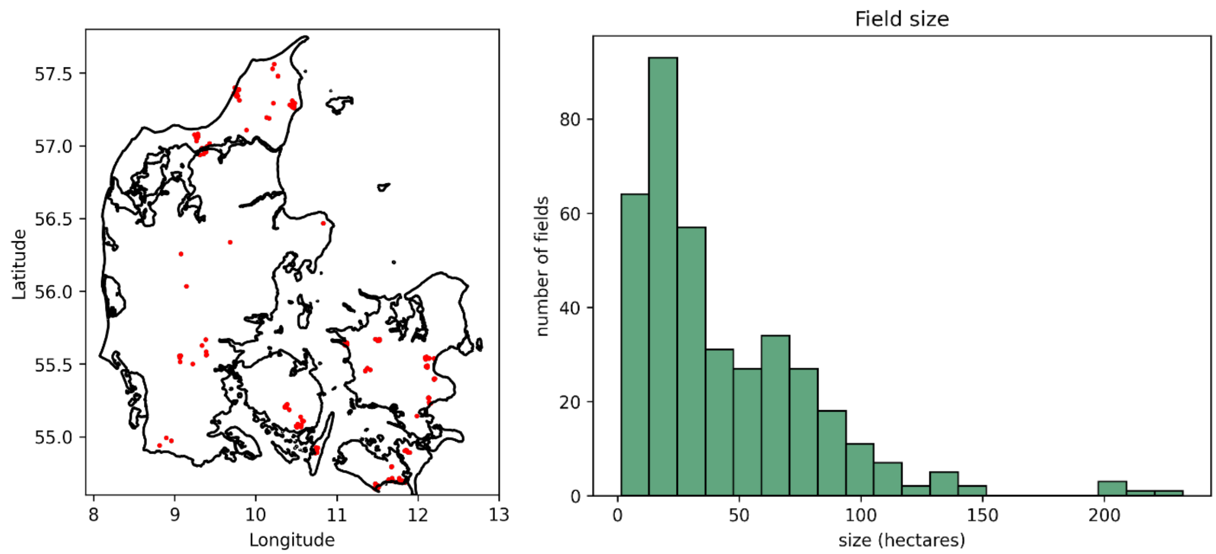

Figure 1. Left: spatial distribution of the studied fields in Denmark. Right: distribution of field size across the winter wheat and spring barley fields.

Datasets

This study makes use of yield, weather, soil, topography and spectral data. A detailed description of each is provided in the following sections, while **Table 1** provides a concise overview of the data.

Yield data

Point-vector yield data were collected for each field from a Danish agricultural company, DanishAgro. Yield observations were obtained from combine harvesters equipped with GPS and yield monitors. We preprocessed the point data by removing biologically infeasible yield as well as statistical outliers. More specifically, all values that fell outside of the 5^{th} and 95^{th} percentiles of the data were considered outliers and discarded.

Next, the point data were rasterized to a 10 m spatial resolution by aligning them with the raster grid from Sentinel-2 and taking the mean yield value across each 10 x 10 m^2 raster cell. The rasterization process is visualized in **Figure 3**. The result is a yield map where each pixel represents the yield in tons per hectare. **Figure 4** shows the pixel-level distribution of yield values across the winter wheat and spring barley fields.

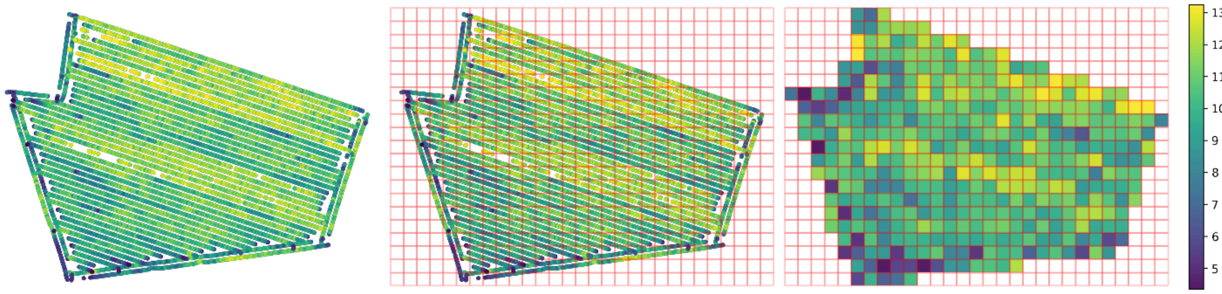

Figure 3. Crop yield rasterization process. Left: the point data of the yield. Center: the point data with the 10 x 10 m^2 raster overlayed. Right: the rasterized yield data, where each raster cell is assigned the mean value of the points that fall within it.

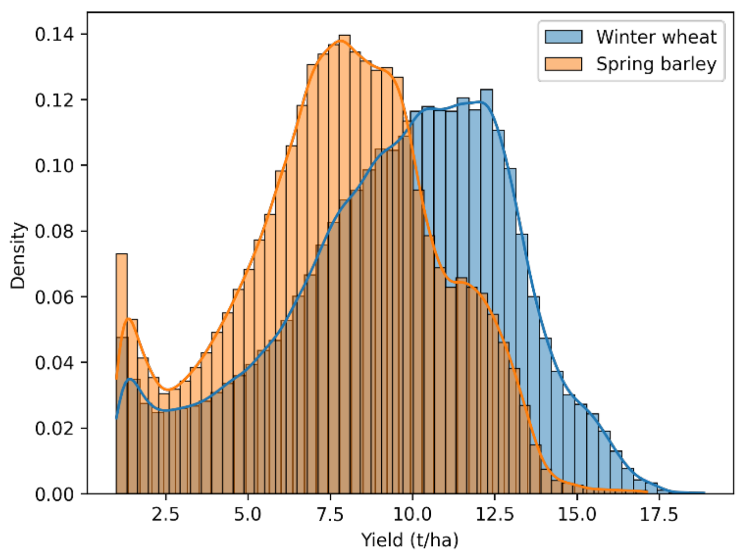

Figure 4. Crop yield distribution at the pixel level (10 m resolution).

Spectral data

Multispectral data were obtained from Sentinel-2, an Earth observation mission from the European Space Agency that collects data at a high spatial resolution of 10 – 60 m and a temporal resolution of approximately 5 days. We make use of 8 spectral bands with 10 – 20 m spatial resolution: red, green and blue (RGB), near infrared (NIR), shortwave infrared (SWIR) 1 and 2, red edge (RE), and scene classification (SCL). To decrease the probability of collecting observations that are obscured by clouds, we filter out any dates with more than 70% cloud coverage. Spectral data were collected between April 1st and May 31st of each year.

Weather data

Weather variables were obtained from TerraClimate (Abatzoglou, et al., 2018), a monthly climate dataset at approximately 4 km gridded resolution. The following 12 variables were selected: minimum temperature (tmin), maximum temperature (tmax), precipitation (ppt), reference evapotranspiration (pet), actual evapotranspiration (aet), wind speed (ws), vapor pressure (vap), vapor pressure deficit (vpd), climate water deficit (def), Palmer Drought Severity Index (PDSI), downward surface shortwave radiation (srad), and snow water equivalent (swe). Data between January and May of each year were obtained.

Soil data

Static soil properties were obtained from SoilGrids (Poggio, et al., 2021) at a spatial resolution of 250 m. This dataset makes use of machine learning to extrapolate global soil properties from ground-based soil measurements and satellite observations. Nine soil properties were selected: bulk density (bd), cation exchange capacity (cec), clay content (clay), nitrogen content (nitrogen), number of coarse fragments (cfvo), pH, sand content (sand), silt content (silt) and soil organic content (soc). Measurements were taken from soil depths of 0 – 5, 5 – 15, and 15 – 30 cm.

Topographic data

Elevation data from the Space Shuttle Radar Topography Mission (SRTM) dataset of NASA (NASA, 2000). This data was measured using an interferometric synthetic aperture radar on the STS-99 mission flown in 2000. The resolution of the data is 30 m.

Table 1. An overview of the data used in this study.

Modality	**Data source**	**Resolution**		**Features**
		Spatial	***Temporal***	
Yield	Combine harvesters	Point	Yearly	Yield in tons per hectare.
Spectral	Sentinel-2	10 m	5 days	RGB, NIR, SWIR 1, SWIR 2, RE, SCL
Weather	TerraClimate	~4 km	Monthly	tmin, tmax, ppt, pet, aet, ws, vap, vpd, def, PDSI, srad, swe
Soil	SoilGrids	250 m	-	bd, cec, clay, nitrogen, cfvo, pH, sand, silt, soc
Topography	SRTM	30 m	-	Elevation

Data preparation

To ensure consistency across data modalities, the collected data are spatially aligned to a 10 m resolution, which matches the highest resolution data from Sentinel-2. Following previous work (Mena, et al., 2025), we apply a cubic spline interpolation to the topographic and soil data, copy the weather value at the field centroid across all field pixels, and use nearest neighbor interpolation to upsample the 20 m spectral data. For the dynamic modalities, i.e. weather and spectral data, we only select observations until May 31st of each year. This is to ensure that in-season predictions approximately 2 – 3 months before harvest can be performed.

The dataset is divided into training, validation and test splits that contain 90, 10, and 10% of the fields, respectively. We perform z-score normalization of the splits based on the statistics computed over the training data. For the training data, we perform random data augmentations in the form of vertical and horizontal flips of the fields.

Model

In this study, the U-Net model (Ronneberger, et al., 2015) is chosen as the crop yield prediction framework. U-Net is a convolutional neural network that contains two phases: contraction, in which the spatial information is reduced while feature information is expanded, and expansion, in which the spatial and feature information are combined through the usage of skip-connection layers. The two-phase setup of the model gives the model its characteristic 'U' shape, after which it is named.

U-Net has commonly been applied to image segmentation tasks, particularly within the biomedical domain. Variations of the model have also been applied to remote sensing data, with applications including the detection of water (Mayer, et al., 2021), clouds (Guo, et al., 2020) and vegetation (Lin, et al., 2023). Beyond classification tasks, U-Net has also been applied to perform regression at the pixel level (Yao, et al., 2018). Moreover, some authors have demonstrated its use for crop yield (Häni, et al., 2020; Mathivanan, et al., 2022; Zhu, et al., 2025).

We implement a U-Net with two encoding-decoding stages as visualized in **Figure 5**. The model is implemented with PyTorch on an Nvidia RTX 1000 GPU. Predictions are made using all multimodal data (spectral, weather, soil and elevation) until the end of May of the respective year, approximately 2 – 3 months before harvest. AdamW is chosen as the optimizer. The hyperparameters are as follows: batch size = 8, learning rate = 10^{-4} and weight decay = 10^{-5}. Training continues until the mean squared error loss converges for both the training and validation split, which typically occurs after 75 epochs. At inference, model performance is evaluated using the coefficient of determination (R^2), root mean squared error (RMSE) and mean absolute error (MAE). The metrics are computed at both the pixel and field level.

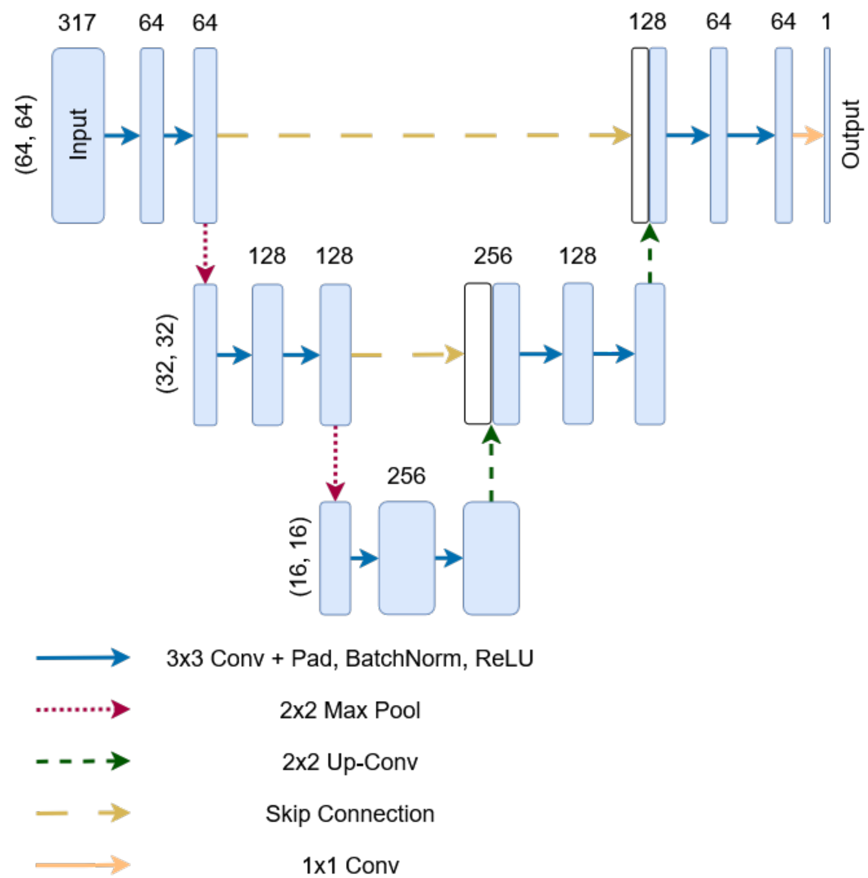

Figure 5. The U-Net model with two encoding-decoding stages that is used in this paper.

Nitrogen monitoring

In this paper, a case study for monitoring nitrogen at the subfield level is provided. The key idea behind our approach is that the difference in **expected** and **predicted** yield can be analyzed to approximate the in-season nitrogen demand across fields. The expected yield is calculated using expert judgments collected in a recent Danish government report (Styrelsen for Grøn Arealomlægning og Vandmiljø, 2025). This document provides information regarding the expected yield output given the target crop and soil type. First, we retrieve the soil type for each field pixel from a 10 m resolution soil type map of Denmark (Møller, et al., 2025). We then compute the corresponding expected yield at each pixel based on the 'yield norm' (Danish: Udbyttenorm) of the target crop, i.e. winter wheat (Danish: Vinterhvede) or spring barley (Danish: Vårbyg). Finally, the **prediction-expectation (PE) yield gap** is calculated as the difference between the predicted and potential yield:

$$\textit{PE yield Gap} = \textit{Predicted Yield} - \textit{Expected Yield}$$

The predicted yield is obtained approximately 2 – 3 months before harvest using the aforementioned U-Net architecture. A positive PE yield gap indicates a higher yield than expected, whereas a negative PE yield gap indicates a lower yield than expected. In the latter case, we hypothesize that there is an increased nitrogen demand and that the area requires more fertilization to achieve its full yield potential. In the results section, a demonstration of this process is provided.

Results

Our analysis includes the validation of the U-Net model performance as well as a demonstration of the nitrogen monitoring approach that has been introduced in this work. **Table 2** shows the quantitative performance analysis of U-Net, where we report the pixel and field level results for all data splits. As expected, performance is highest on the training data, yet model performance only decreases slightly on the validation and test splits. This indicates that the model generalizes well to unseen data.

Table 2. Crop yield prediction performance of the U-Net model. R^2, RMSE, and MAE are reported at the pixel level (i.e. subfield) and field level.

Data split	***Pixel level***			***Field level***		
	R^2	**RMSE**	**MAE**	**R^2**	**RMSE**	**MAE**
Training	0.576	1.878	1.474	0.887	0.751	0.621
Validation	0.530	2.010	1.544	0.782	1.085	0.852
Test	0.506	2.186	1.702	0.751	1.213	0.985

Next, a qualitative analysis of the model's performance is conducted for an example field. The crop type of the chosen field is spring barley, and it was harvested in 2024. **Figure 6** shows the true yield data, the U-Net predictions, and the error in prediction compared to the true labels. The RMSE is 0.937 and 1.740 at the field and pixel level, respectively, which we find to be a relatively low prediction error. We therefore conclude that the U-Net model provides a reliable yield estimation for the given field.

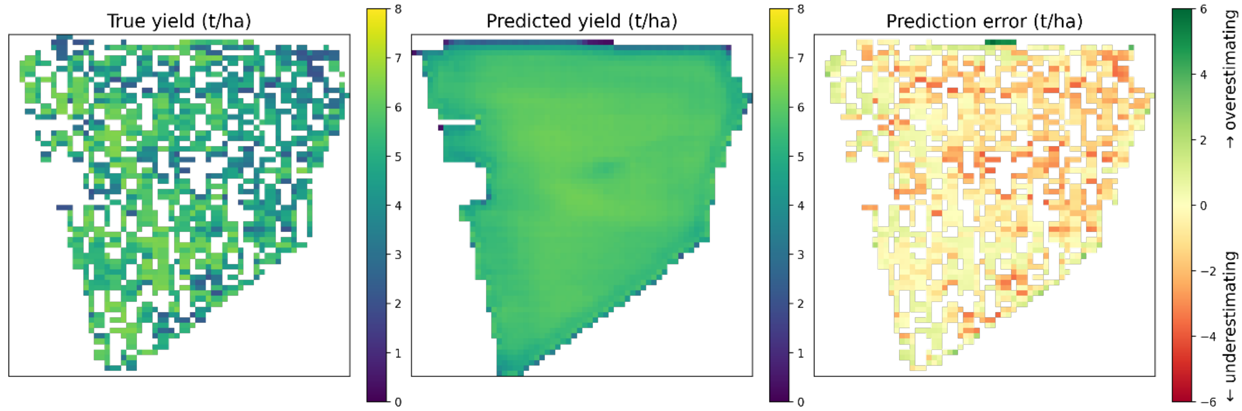

Figure 6. Qualitative analysis of the U-Net model performance on an example field. Left: true yield data that was harvested in August. Center: in-season predictions made by U-Net at the end of May. Right: prediction error of the U-Net model.

Our nitrogen monitoring approach is demonstrated in **Figure 7**. The example spring barley field contains various soil types, and the expected yield is higher in regions rich in clay (~7 t/ha) while it is lower in those containing more sand or humus (~5.5 t/ha). The predicted yield, in contrast, is homogeneous across the field (~5.5 t/ha).

We observe that the clay-rich regions in the field show a negative PE yield gap, indicating that yield is below its expected value and that nitrogen demands are not met. In contrast, the PE yield gap in the sandy regions is close to zero, indicating that nitrogen demands are met. In Denmark, fixed-rate applications of fertilizer across fields based on the dominant field type are common. As such, variations in nitrogen demand, and hence yield potential, are not considered. Our example indicates that fertilization was optimized for sandy soil, the dominant soil type of the barley field, and this led to suboptimal fertilization and yield for the clay-rich regions. Precision fertilization would allow for clay-rich areas in the field to receive more fertilizer, thus resulting in higher yield output than current practices.

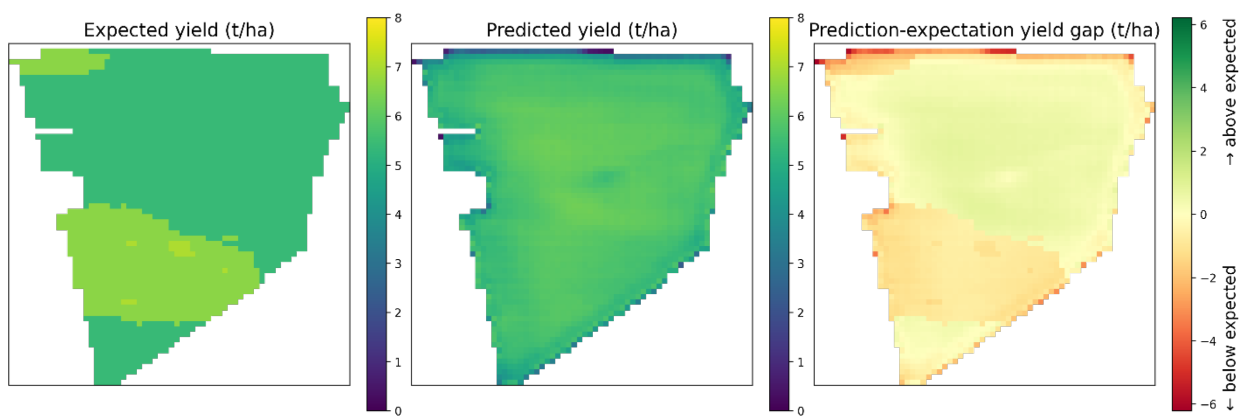

Figure 7. Nitrogen monitoring approach demonstrated on an example field. Left: the expected yield as calculated from expert judgments. Center: predictions made by U-Net. Right: the PE yield gap between the predicted and expected yield, which indicates nitrogen demands.

Conclusion

This paper introduced a novel approach for monitoring nitrogen at the subfield level. Data for over 350 winter wheat and spring barley fields across Denmark were collected to demonstrate how nitrogen requirements can be estimated in a timely manner, enabling precise adjustments of fertilizer application within individual fields. The key idea behind the approach is that the difference between predicted and expected crop yield can be used to approximate nitrogen demands.

A U-Net model was implemented to provide in-season crop yield predictions approximately 2 – 3 months before harvest at a 10 x 10 m^2 pixel scale. The model leveraged various data sources, in particular spectral, weather, soil and topographical data. At the pixel level, a R^2 of 0.576/0.530/0.506, RMSE of 1.878/2.010/2.186 and MAE of 1.474/1.544/1.702 were achieved on the train/validation/test data, demonstrating robust performance across all data splits and strong generalization to unseen data.

Judgments from Danish experts were consulted to calculate the expected yield. Calculations considered the crop type and soil texture across the fields. The difference between the predicted and expected yield is defined as the **prediction-expectation (PE) yield gap**, which we use as a proxy for the nitrogen demand. Our approach was demonstrated on an example field, and results indicated that clay-rich areas received suboptimal fertilization. Precision fertilization based on our approach would improve yield overall while increasing fertilization only where needed, rather than uniformly applying a static fertilizer rate across the entire field.

While our approach showed promising results, some limitations must be noted. In addition to nitrogen availability, yield is impacted by parameters such as water stress and other biotic and abiotic stressors. These factors should also be considered when interpreting the gap between the expected and predicted yield. As data on these stressors was not available for our case study, we leave their incorporation to future work.

Accurate yield predictions are critical for the practical implementation of the proposed approach, and further improvements can be made with regard to the current methodology. The incorporation of finer-grained multimodal data, as well as the collection of more yield data across locations and time periods, will help improve model performance. Although initial experiments with other model architectures did not prove fruitful for our setup, we recommend future work to further explore alternative models that may be suitable when applying our framework to other crops, regions and expert judgments.

Ultimately, the central contribution of this work is not specific model choices or the calculations of expected yield from expert judgments. These components merely serve to illustrate how the proposed approach for nitrogen monitoring can be applied in practice. We hope our approach can be adopted for a broader range of contexts and provide a foundation for future nitrogen monitoring applications.

Acknowledgments

This work was supported by The Innovation Fund Denmark [grant number 1152-00017A - FOFE - Foliar fertilization for a more efficient, environmental, and climate friendly crop production]. This work was also supported by the VILLUM Young Investigator 2024 project (00072051), the Novo Nordisk Starting Grant (NNF23OC0087612), and the SCALE project (Food and Bio Cluster, Innovation Fund Denmark).

References

Abatzoglou, J., Dobrowski, S., Parks, S., & Hegewisch, K. (2018). TerraClimate, a high-resolution global dataset of monthly climate and climatic water balance from 1958–2015. *Scientific data, 5*(1), 170191.

Balasubramanian, V., Alves, B., Aulakh, M., Bekunda, M., Cai, Z., Drinkwater, L., . . . Oenema, O. (2004). Crop, environmental, and management factors affecting nitrogen use efficiency. *Agriculture and the nitrogen cycle, 65*, 19-33.

Guo, J., Zhao, H., Tan, H., Wang, Y., & Yan, H. (2026). Multisource data and multitask deep learning for predicting alfalfa growth indicators. *Precision Agriculture, 27*(2), 45.

Guo, Y., Cao, X., Liu, B., & Gao, M. (2020). Cloud detection for satellite imagery using attention-based U-Net convolutional neural network. *Symmetry, 12*(6), 1056.

Häni, N., Roy, P., & Isler, V. (2020). Häni, N., Roy, P., & Isler, V. (2020). A comparative study of fruit detection and counting methods for yield mapping in apple orchards. *Journal of Field Robotics, 37*(2), 263-282.

Hu, J., Sheng, L., & Sun, G. (2018). Squeeze-and-excitation networks. *Proceedings of the IEEE conference on computer vision and pattern recognition.* (pp. 7132-7141). Salt Lake City, United States: IEEE.

Kumhálová, J., Kumhála, F., Kroulík, M., & Matějková, Š. (2011). The impact of topography on soil properties and yield and the effects of weather conditions. *Precision Agriculture*, 813--830.

Lin, N., Quan, H., He, J., Li, S., Xiao, M., Wang, B., . . . Li, N. (2023). Urban vegetation extraction from high-resolution remote sensing imagery on SD-UNet and vegetation spectral features. *Remote Sensing, 15*(18), 4488.

Lin, Z., Wang, S., Guan, K., Zhang, J., Asseng, S., Gislum, R., . . . Zhou, R. (2026). TMF: Temporal multi-modal fusion framework for estimating wheat yield from multi-source satellite and environmental data across the European Union. *ISPRS Journal of Photogrammetry and Remote Sensing, 239*, 147-163.

Mathivanan, S. K., & Jayagopal, P. (2022). Utilizing satellite and UAV data for crop yield prediction and monitoring through deep learning. *Acta Geophysica, 70*(6), 2991-3004.

Mayer, T., Poortinga, A., Bhandar, B., Nicolau, A., Market, K., Thwal, N. S., . . . Saah, D. (2021). Deep learning approach for Sentinel-1 surface water mapping leveraging Google Earth Engine. *ISPRS Open Journal of Photogrammetry and Remote Sensing, 2*, 100005.

Mena, F., Pathak, D., Najjar, H., Sanchez, C., Helber, P., Bischke, B., . . . Charfueland, M. (2025). Adaptive fusion of multi-modal remote sensing data for optimal sub-field crop yield prediction. *Remote Sensing of Environment, 318*, 114547.

Møller, A. B., Nyborg, L., Grogan, K., Druce, D., Svane, S. F., Greve, M. B., . . . Beucher, A. (2025). High-resolution 3D soil texture mapping in Denmark using satellite time series and bare soil composites. *Advances in Agronomy, 194*, 133-186.

NASA. (2000, February 1). *SRTM*. Retrieved June 8, 2026, from EarthData: https://www.earthdata.nasa.gov/data/instruments/srtm

Poggio, L., Sousa, L. D., Batjes, N., Heuvelink, G., Kempen, B., Ribeiro, E., & Rossiter, D. (2021). SoilGrids 2.0: producing soil information for the globe with quantified spatial uncertainty. *Soil, 7*(1), 217-240.

Ronneberger, O., Fischer, P., & Brox, T. (2015). U-net: Convolutional networks for biomedical image segmentation. *Medical Image Computing and Computer-Assisted Intervention* (pp. 234-241). Munich: Springer international publishing.

Styrelsen for Grøn Arealomlægning og Vandmiljø. (2025). *Vejledning om gødsknings- og harmoniregler.* Copenhagen, Denmark: Ministeriet for Grøn Trepart.

Wang, S., Guan, K., Wang, Z., Ainsworth, E., Zheng, T., Townsend, P., . . . Wu, G. (2021). Airborne hyperspectral imaging of nitrogen deficiency on crop traits and yield of maize by machine learning and radiative transfer modeling. *International Journal of Applied Earth Observation and Geoinformation, 105*, 102617.

Yao, W., Zeng, Z., Lian, C., & Tang, H. (2018). Pixel-wise regression using U-Net and its application on pansharpening. *Neurocomputing, 312*, 364-371.

Zhou, Y., Ata-Ul-Karim, S., Yin, J., Tóth, L., Wang, S., Ma, Y., . . . Cammarano, D. (2026). Assessing in-season crop nitrogen status based on UAV multispectral imaging and AI-driven model optimization. *Computers and Electronics in Agriculture*, 111638.

Zhou, Y., Ma, Y., Ata-Ul-Karim, S., Wang, S., Ciampitti, I., Antoniuk, V., . . . Cammarano, D. (2025). Integrating multi-angle and multi-scale remote sensing for precision nitrogen management in agriculture: A review. *Computers and Electronics in Agriculture, 230*, 109829.

Zhu, Z., Chen, Y., Lu, C., Yang, M., Xia, Y., Huang, D., & Lv, J. (2025). Research on Crop Classification Using U-Net Integrated with Multimodal Remote Sensing Temporal Features. *Sensors, 25*(16), 5005.